View metadata, citation and similar papers at core.ac.uk

brought to you by CORE

provided by Aston Publications Explorer

PROCEEDINGS OF SPIE

SPIEDigitalLibrary.org/conference-proceedings-of-spie

Rogue waves driven by polarization instabilities in a long ring fiber oscillator

S. A. Kolpakov, Hani Kbashi, Sergey Sergeyev

SPIE.

Downloaded From: https://www.spiedigitallibrary.org/conference-proceedings-of-spie on 11/2/2017 Terms of Use: https://spiedigitallibrary.spie.org/ss/TermsOfUse.aspx

Rogue Waves Driven by Polarization Instabilities in a Long Ring Fiber Oscillator

S. A. Kolpakov[a], Hani Kbashi[a], and Sergey Sergeyev[a]

[a]School of Engineering and Applied Science, Aston University, Aston Triangle, Birmingham, B4 7ET, UK

ABSTRACT

We present an experimental and theoretical results of a study of a complex nonlinear polarization dynamics in a passively self-mode-locked erbium-doped fiber oscillator implemented in a ring configuration and operating near lasing threshold. The theoretical model consists of seven coupled non-linear equations and takes into account both orthogonal states of polarizations in the fiber. The experiment confirmed the existence of seven eigenfrequencies, predicted by the model due to polarization instability near lasing threshold. By adjusting the state of polarization of the pump and in-cavity birefringence we changed some eigenfrequencies from being different (non-degenerate state) to matching (degenerate state). The non-degenerate states of oscillator lead to the L-shaped probability distribution function and true rogue wave regime with a positive dominant Lyapunov exponent value between 1.4 and 2.6. Small detuning from partially degenerate case also leads to L-shaped probability distribution function with the tail trespassing eight standard deviations threshold, giving periodic patterns of pulses along with positive dominant Lyapunov exponent of a filtered signal between 0.6 and 3.2. The partial degeneration, in turn, guides to quasi-symmetric distribution and the value of dominant Lyapunov exponent of 42 which is a typical value for systems with a source of the strongly nonhomogeneous external noise.

Keywords: Optical rogue wave, rogue wave, fiber laser, polarization instability degeneration, non-degenerate states, chaos, chaos transition

1. INTRODUCTION

Previously, it was shown theoretically and confirmed experimentally that a possible scenario of the emergence of rogue wave (RW) events in lasers is a pulse-pulse interaction (see 1 for a detailed description of observed RW patterns). These interactions were claimed to have a chaotic dynamics, although experimentally this claim was not proven. The role played by noise in RW generation, in our opinion, still remains unclear, although some investigators claimed the importance of a noisy seed to formation of RW patterns (2, 3).

The wave chaos was observed using microwaves in experiments with metallic cavities. These systems were described using differential equations similar to Schrdinger and Helmholtz equations (see for example a case of flat metallic cavity 4). The experimental results 5 proved that this 3-D electromagnetic problem is similar to the universal laws of a quantum chaos theory. From one hand this studies shown that the aforesaid chaotic behavior 6 can be a manifestation of a universal law of nature due to the system behavior does not depend on the particular geometry of the system. From another hand, the main drawback of aforementioned attempts is the presence of a virtually infinite number of eigenstates 7. This intrinsic complexity of the aforementioned systems and lack of control over the number of eigenstates does not allow a detailed study of the transition of a system from a non-chaotic to chaotic behavior.

In aforementioned context, a fiber laser oscillator, i.e. ring cavity without saturable absorber is a good choice, due to a limited number of eigenstates as well as the possibility to change the number of excited eigenstates in the experiment. The main difference of these devices from hollow metallic cavities is that the electromagnetic wave has only one mode and one direction of propagation, meanwhile, the polarization of it plays the role of another two dimensions. Hence the system of equations describing the system is simple and easy to handle. The

Further author information: (Send correspondence to S. A. Kolpakov)
S. A. Kolpakov: E-mail: stanisalv.kolpakov@gmail.com

Nonlinear Optics and Applications X, edited by Mario Bertolotti, Joseph W. Haus, Alexei M. Zheltikov, Proc. of SPIE Vol. 10228, 102280Q · © 2017 SPIE · CCC code: 0277-786X/17/$18 · doi: 10.1117/12.2265190

Downloaded From: https://www.spiedigitallibrary.org/conference-proceedings-of-spie on 11/2/2017 Terms of Use: https://spiedigitallibrary.spie.org/ss/TermsOfUse.aspx

oscillator has seven eigenfrequencies which appear due to polarization instability near lasing threshold. During the experiment, the polarization can be easily changed using polarization controllers to change the grade of degeneration of the oscillating system. Another advantage is a possibility to record a long dataset in few seconds and digitally filter the data set using a build in the low bandpass filter.

Generation of chaotic regimes we address to a new type of the low threshold vector resonance multimode instability (VRMI) [8] which inherits features of both multimode and modulation instabilities. In the same fashion as for the previously known multimode instabilities, a large number of longitudinal modes is excited without synchronization. To enable VRMI, we modulated the state of polarization of the signal with the period of beating length between modes with two orthogonal polarizations changing the in-cavity birefringence and the state of polarization of the pump wave. As a result, we observed the gradual transition from the noisy chaotic regime through different self-pulsing regimes with positive dominant Lyapunov exponent (MLE) to the true RW regimes [1].

2. THEORETICAL BACKGROUND

Following rate equations were derived in [8]:

$$\frac{\partial S_0}{\partial z}+\frac{\partial S_0}{\partial t}=\left(\frac{2\alpha_1 f_1}{1+\Delta^2}-2\alpha_2\right)S_0+\frac{2\alpha_1 f_2}{1+\Delta^2}S_1+\frac{2\alpha_1 f_3}{1+\Delta^2}S_2, \tag{1}$$

$$\frac{\partial S_1}{\partial z}+\frac{\partial S_1}{\partial t}=\gamma S_2 S_3+\left(\frac{2\alpha_1 f_1}{1+\Delta^2}-2\alpha_2\right)S_1+\frac{2\alpha_1 f_2}{1+\Delta^2}S_0-\frac{2\alpha_1 f_3\Delta}{1+\Delta^2}S_3, \tag{2}$$

$$\frac{\partial S_2}{\partial z}+\frac{\partial S_2}{\partial t}=-\gamma S_1 S_3+\frac{2\alpha_1 f_3}{1+\Delta^2}S_0+\left(\frac{2\alpha_1 f_1}{1+\Delta^2}-2\alpha_2\right)S_2+\left(\frac{2\alpha_1 f_2\Delta}{1+\Delta^2}-2\beta\right)S_3, \tag{3}$$

$$\frac{\partial S_3}{\partial z}+\frac{\partial S_3}{\partial t}=\frac{2\alpha_1\Delta f_3}{1+\Delta^2}S_1-\frac{2\alpha_1\Delta f_2}{1+\Delta^2}S_2+2\beta S_2+\left(\frac{2\alpha_1 f_1}{1+\Delta^2}-2\alpha_2\right)S_3, \tag{4}$$

$$\frac{df_1}{dt}=\varepsilon\left[\frac{(\chi_s-1)I_p}{2}-1-\left(1+\frac{I_p\chi_p}{2}+d_1S_0\right)f_1-\left(d_1S_1+\frac{I_p}{2}\xi\right)f_2-d_1S_2f_3\right], \tag{5}$$

$$\frac{df_2}{dt}=\varepsilon\left[l\xi\frac{I_p(\chi_s-1)}{4}-\left(\frac{I_p\chi_p}{2}+1+d_1S_0\right)f_2-\left(\frac{I_p\chi_p}{2}\xi+d_1S_1\right)\frac{f_1}{2}\right], \tag{6}$$

$$\frac{df_3}{dt}=-\varepsilon\left[\frac{d_1S_2f_1}{2}+\left(\frac{I_p\chi_p}{2}+1+d_1S_0\right)f_3\right], \tag{7}$$

Here time is normalized to the round trip and distance - to the cavity length; S_i(i=0,1,2,3) are Stokes parameters, normalized to the saturation power: ${S_0}^2={S_1}^2+{S_2}^2+{S_3}^2$); α_1 is the total absorption of erbium ions at the lasing wavelength, α_2 is the total insertion losses in cavity, β is the birefringence strength ($2\beta=2\pi L/L_b$ where L_b is the beat length); $\xi=(1-\delta^2)/(1+\delta^2)$ is parameter of the pump anisotropy, Δ is the ellipticity of the pump wave, $\varepsilon=\tau_R/\tau_{Er}$, τ_R is the round trip time and τ_{Er} is the lifetime of the first level; ${\chi_{p,s}}=({\sigma_a}^{(s,p)}+{\sigma_e}^{(s,p)})/{\sigma_a}^{(s,p)}$, ${\sigma_{a,e}}^{(s,p)}$ are absorption and emission cross sections at the lasing (s) and pump (p) wavelengths Δ is the detuning of the lasing wavelength from the maximum of the gain spectrum normalized to the width of it; $d_1=\chi/\pi(1+\Delta^2)$ and f_i $(i=1,2,3)$ are related to the angular distribution of the excited ions $n(\theta)$ expanded into Fourier series [8].

Equations (1) - (7) were derived assuming that the dipole moments of the absorption and emission transitions for erbium doped silica are located in the plane orthogonal to the direction of propagation. In the experiments, we set the pump power at 18 mW which is significantly less than the power (~800 mW) required for mode locking based on nonlinear polarization rotation [9]. The average length of pulses in the experiments was measured to be

Downloaded From: https://www.spiedigitallibrary.org/conference-proceedings-of-spie on 11/2/2017 Terms of Use: https://spiedigitallibrary.spie.org/ss/TermsOfUse.aspx

of ∼10 ns which is much longer than the time of transverse relaxation (∼160 fs). Hence, in this approximation the second order dispersion was dropped as well as the dynamics of polarization in silica.

To find conditions for VRMI, we linearized Eqs. (1) - (7) in the vicinity of the steady state solution $\boldsymbol{F}_0=(S_{00}\pm S_{00}\ 0\ 0\ f_{10}\ f_{20}\ 0)^T$ and find eigenvalues as follows:

$$\lambda_0 = iq + A_0\left(I_p, \xi\right), \tag{8}$$

$$\lambda_1 = A_1\left(q, I_p, \xi\right) + i\Omega_1\left(q, I_p, \xi\right), \tag{9}$$

$$\lambda_2 = A_2\left(q, I_p, \xi\right) + i\Omega_2\left(q, I_p, \xi\right), \tag{10}$$

$$\lambda_3 = A_3\left(q, I_p, \xi\right) + i\Omega_3\left(q, I_p, \xi\right), \tag{11}$$

$$\lambda_4 = A_4\left(q, I_p, \beta, \xi\right) + i\Omega_4\left(q, I_p, \beta, \zeta\right), \tag{12}$$

$$\lambda_5 = A_5\left(q, I_p, \beta, \xi\right) + i\left(q + \Delta\Omega\left(q, I_p, \beta, \xi\right)\right), \tag{13}$$

$$\lambda_6 = A_6\left(q, I_p, \beta, \xi\right) + i\left(q - \Delta\Omega\left(q, I_p, \beta, \xi\right)\right), \tag{14}$$

$$\lambda_6 = A_6\left(q, I_p, \beta, \xi\right) + i\left(q - \Delta\Omega\left(q, I_p, \beta, \xi\right)\right), \tag{15}$$

Here $q=0,\pm1,\ \pm2,..\pm N$ are wave numbers of the longitudinal modes. All eigenvalues were normalized to the fundamental frequency $\omega=2\pi/\tau_R$.

3. EXPERIMENTAL SETUP

The schematic of experiment is illustrated in Fig. 1. An unidirectional ring cavity with a single polarization controller inside it to regulate in-cavity birefringence was assembled using 1 m of Er3+ doped fiber *Liekki Er80-8/125* and 614 m of a single-mode fiber *SMF-28* ($\beta_2=-21ps^2/km$). Whole cavity length was of 615 m to ensure tuning of non-degenerate regimes (achieve full degeneration in a short cavity is impossible because of interaction between acoustic and optic modes in fibre).

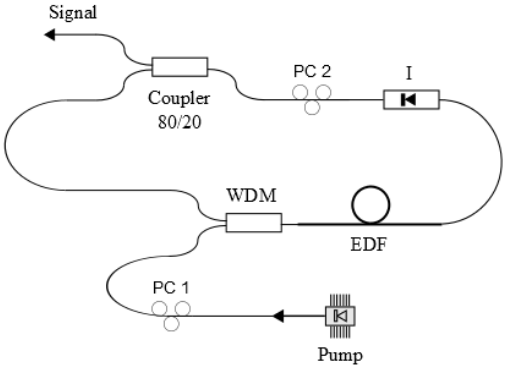

Figure 1. Schematic of the laser oscillator.

Downloaded From: https://www.spiedigitallibrary.org/conference-proceedings-of-spie on 11/2/2017 Terms of Use: https://spiedigitallibrary.spie.org/ss/TermsOfUse.aspx

Polarization insensitive optical isolator (labeled with "I" in Fig. 1) with the attenuation ratio of 51dB was used to completely suppress a back-propagated wave in the cavity. The 80/20 fiber coupler was installed to sample a portion of the signal wave. The cavity was pumped via a 1480/1550 WDM, using a 1480 nm laser diode *FOL14xx* series with built-in optical isolator. The supplied pump power was measured after the pump polarization controller (PC1) and the wavelength division multiplexing (WDM) just before the Er^{3+} doped fiber. The signal was detected using an *InGaAs UDP-15-IR-2-FC* detector with the bandwidth of 17 GHz connected to the 2.5 GHz sampling oscilloscope *Tektronix DPO7254*. Optical spectrum analyzer (OSA) *Yokogawa AQ6317B* was used to record the optical spectra of the signal; polarimeter *Thorlabs IPM5300* was employed to measure the Stokes parameters of the signal wave. Radio frequency (RF) analyzer has the bandwidth of 13.5 GHz. The angles of polarization controllers were measured relatively to the vertical position of the knob.

4. EXPERIMENTAL RESULTS

4.1 Threshold and radio frequency spectra

The fiber oscillator has a lasing threshold of 16 mW, calculated from the curve of output versus pump power shown in the left inset in Fig. 2. After measuring it we set the pump power at 18.4 mW. At this regime, the polarization dependent instabilities which appear close to the lasing threshold were clearly observable. The pump power remained constant during all set of experiments. The output power was measured to be of 1.2 mW for all the set of experiments.

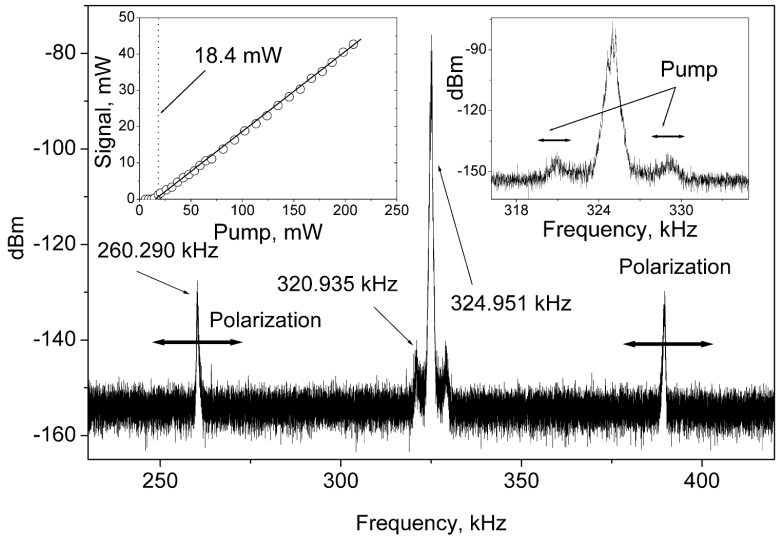

Figure 2. Main frame: RF spectrum showing peak for harmonics ν_0 (324,9 kHz, round-trip), ν_1 (260,3 and 389,5 kHz, polarization dependent) and ν_2 (320,9 and 329.9 kHz, which is pump power dependent one); left insert: signal/pump curve and the lasing threshold, right insert: amplified area about ν_0 and ν_2.

Two groups of oscillation regimes were observed in a long oscillator, a degenerate one having three first eigenfrequencies and non-degenerate one showing all seven eigenfrequencies. The RF spectra for both scenarios are illustrated in the main frame of Fig. 2 and Fig. 3.

Evolution of the polarization dependent satellites as a function of the angle of the knob of PC2 is illustrated in Fig. 4a. The frequency offset of these satellites (ν_2) depends on the pump power as illustrated in Fig. 4b, and this variation can be fitted with the equation shown in Fig. 4b. The gap just before the lasing threshold (see the encircled area) in the curve can be explained by the transition between a single-frequency (only pump wavelength) and double-frequency (the pump and signal wavelengths) regimes.

Downloaded From: https://www.spiedigitallibrary.org/conference-proceedings-of-spie on 11/2/2017 Terms of Use: https://spiedigitallibrary.spie.org/ss/TermsOfUse.aspx

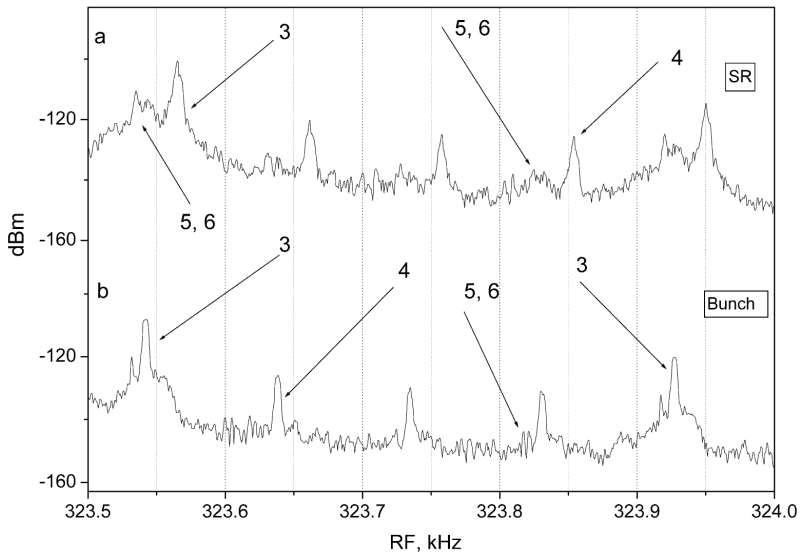

Figure 3. Frequencies ν_3 (385 Hz), ν_4 (97 Hz), ν_5 and ν_6 (30 and 20 Hz respectively) observed for non-degenerate states of the oscillator.

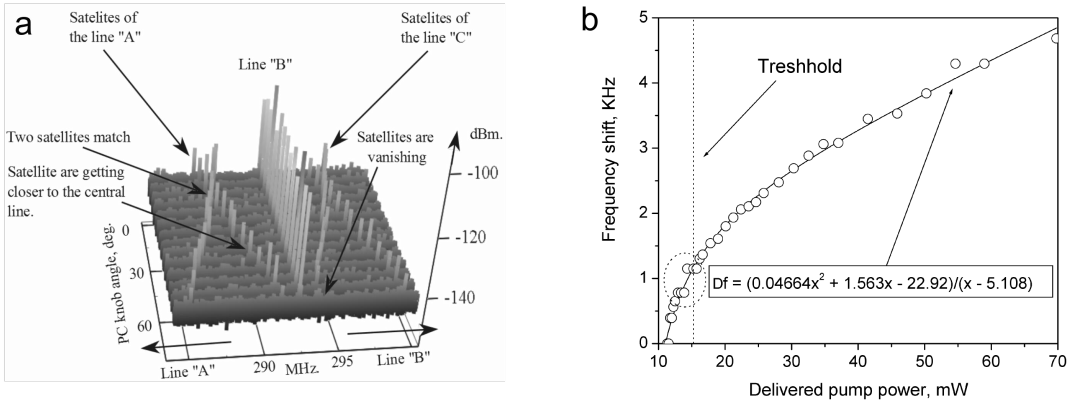

Figure 4. Right insert: evolution of ν_1 as a function of induced birefringence; left insert: distances between pump depending satellites (ν_2)and the central RF line (ν_0) as a function of the pump power.

4.2 Regimes of oscillations and polarization dynamics

Change of the position of the knob of PC2 resulted in different oscillation regimes (Fig. 5 - 10). At $-90°$ the laser operated in a noisy regime (NR) (Fig. 5 a). In this case, no regular pulsations were observed in the oscilloscope trace or in IPM. The probability distribution function (PDF) of the signal power has a symmetric shape (-shape) (Fig. 11a). The value of the dominant Lyapunov exponent (MLE) 10 for oscilloscope trace was estimated to be 42. This value indicated the presence of a strong noise modulation of pump 1. After filtering the signal with the low band pass filter with the width of 1MHz the value of MLE was estimated to be of 0.35 this value indicates a chaotic regime close to random walk.

Self-mode locking at fundamental frequency was observed when the knob of PC2 was set at $-80°$ (see Fig. 5 b). In these conditions, the pulse width was measured to be of $\sim$40 ns. The period of pulsations was calculated from the oscilloscope trace to be of 3.077 s, matching with the fundamental frequency of 325.2 kHz (ν_0), measured

Downloaded From: https://www.spiedigitallibrary.org/conference-proceedings-of-spie on 11/2/2017 Terms of Use: https://spiedigitallibrary.spie.org/ss/TermsOfUse.aspx

from RF. The RF spectra for this regime was different from the RF spectra for the noisy regime (compare 6a and 6b), two small satellites were observed at the distance 100 Hz from the polarization dependent lines. At the same time, the position of the polarization dependent (ν_1) satellites was changed as well as the position of the optical line (see Fig. 7 b).

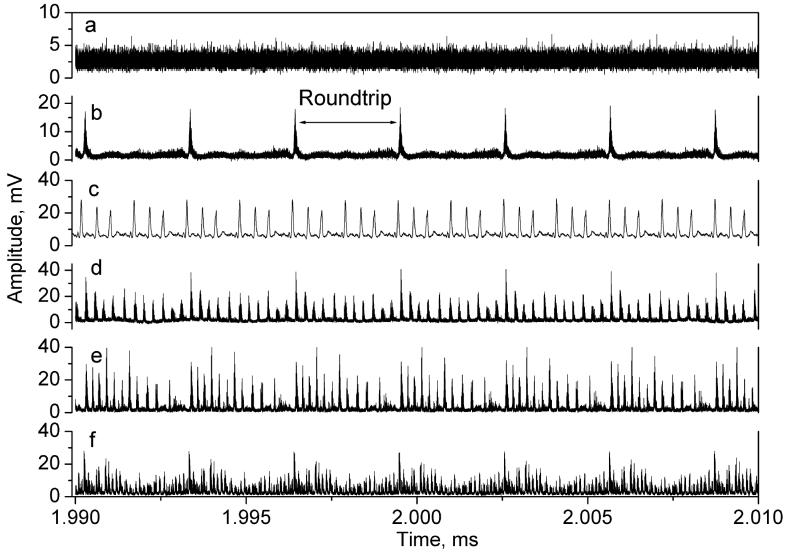

Figure 5. Oscilloscope traces for different regimes; a-noisy regime, b-self-mode-lock; c-five pulses; d-ten pulses; e-the regime similar to soliton rain and f-bunch of pulses.

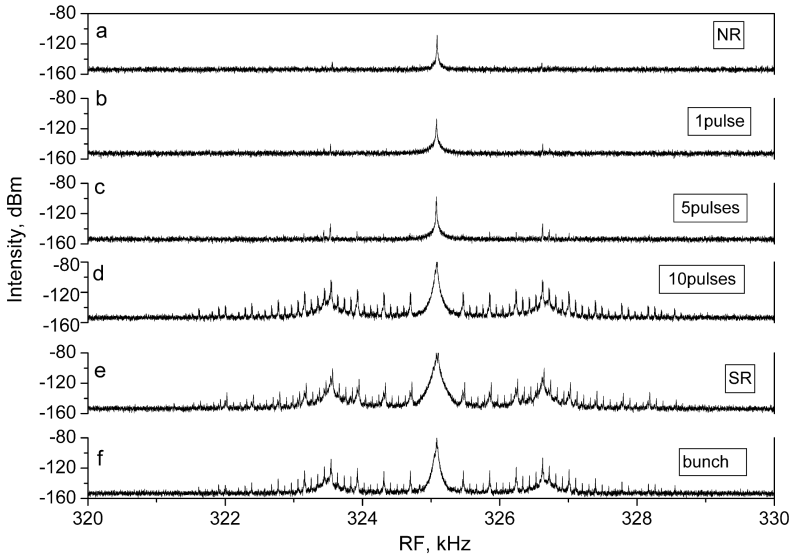

Figure 6. . Comparison of RF spectra for different regimes; a- noisy regime, b-self-mode-lock; c-five pulses; d-ten pulses; e-the regime similar to soliton rain and f-bunches of pulses.

Also, the OSA spectrum showed the existence of one polarization in the cavity. The behavior of Stocks parameters was chaotic for all three parameters (see Figs. 8b - 10b and 1). The portion of a noisy component

Downloaded From: https://www.spiedigitallibrary.org/conference-proceedings-of-spie on 11/2/2017 Terms of Use: https://spiedigitallibrary.spie.org/ss/TermsOfUse.aspx

decreased meanwhile the value of MLE for filtered signal and Stocks parameters was > 3. Also, the PDF for this regime was drastically different from the first case (compare Figs. 11a and 11b). The shape of it became L- like. Frequently this shape was addressed to the existence of RW in the system and chaos, although in this particular case the oscillations were predictable and the value of MLE was positive rather due to strong noise modulation of Stocks parameters than to a chaotic signal itself. After further digital filtering of the signal MLE decreased below zero.

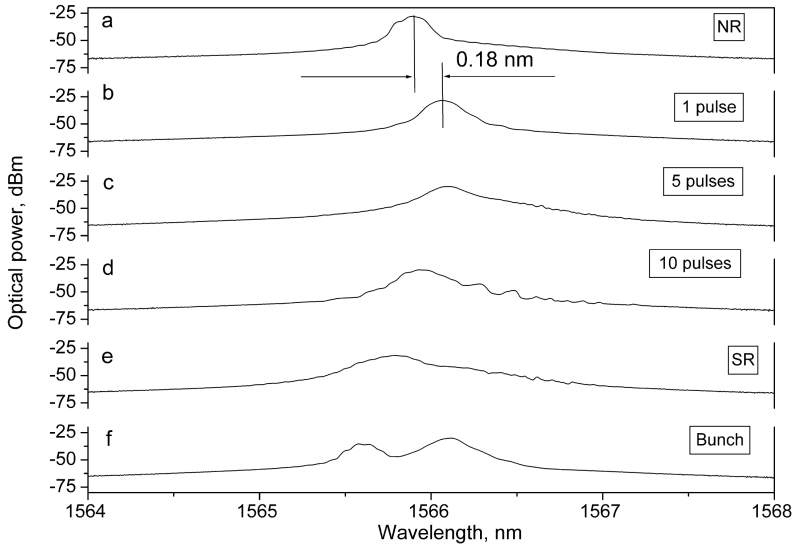

Figure 7. Optical spectra for different regimes; a - noisy regime, b -self-mode-locked; c-five pulses; d - ten pulses; e - the regime similar to soliton rain and f - bunches of pulses.

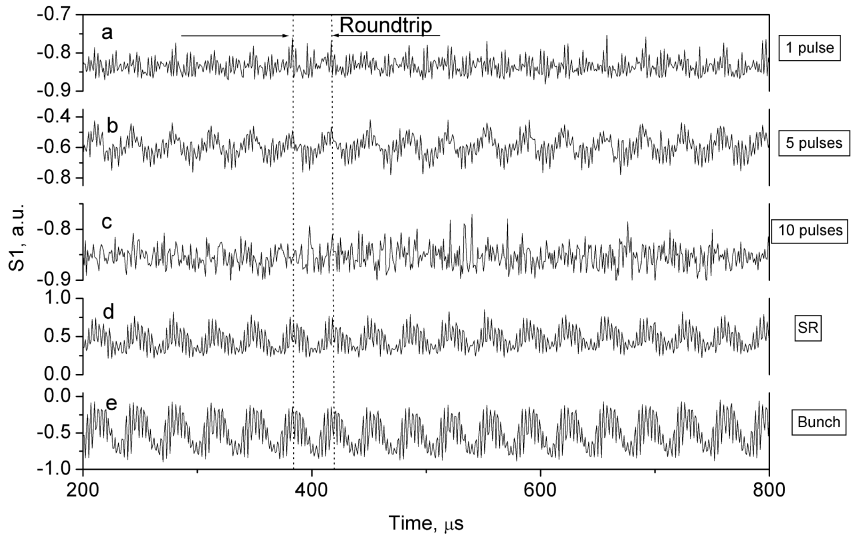

Figure 8. Dynamics of the normalized Stokes parameters s1 for different regimes: a - self-mode-lock; b -five pulses; c - ten pulses; d - the regime similar to soliton rain and e - bunches of pulses.

Downloaded From: https://www.spiedigitallibrary.org/conference-proceedings-of-spie on 11/2/2017 Terms of Use: https://spiedigitallibrary.spie.org/ss/TermsOfUse.aspx

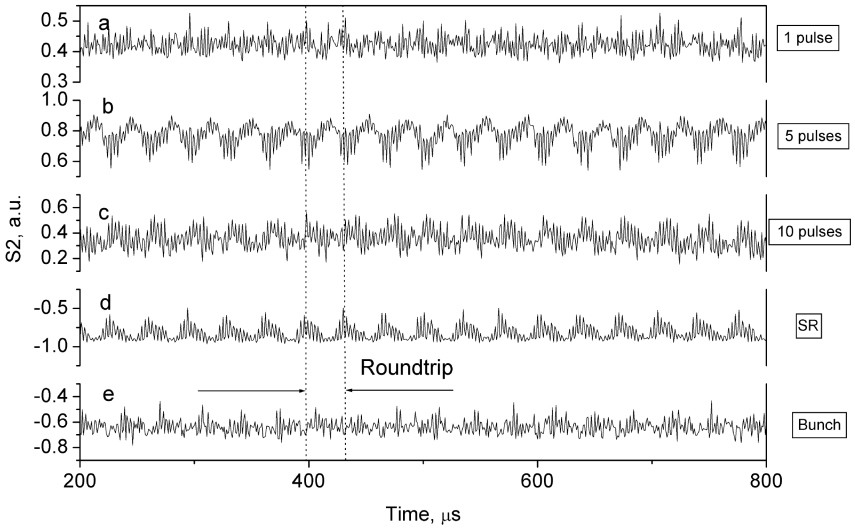

Figure 9. Dynamics of the normalized Stokes parameters s2 for different regimes: a - self-mode-lock; b - five pulses; c - ten pulses; d - the regime similar to soliton rain and e - bunches of pulses.

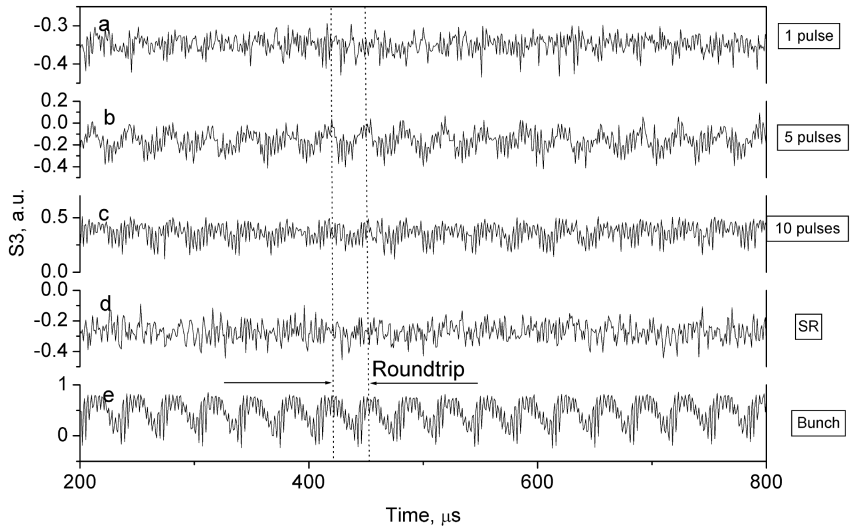

Figure 10. Dynamics of the normalized Stokes parameters s3 for different regimes: a - self-mode-lock; b - five pulses; c - ten pulses; d - the regime similar to soliton rain and e - bunches of pulses.

In this case, noise pulses were surpassing the threshold of eight standard deviations from the mean value. Noise envelope of the pulses made the PDF smooth. This kind of events can be technically considered as fast RWs, but taken into account the periodicity of these events, they would be classified in a subclass of periodic events with L-shaped statistics rather than true RWs. Summarizing, when the system was slightly detuned from the degenerate state, we observed predictable events with L-shaped statistics. The regime with five pulses illustrated in Figs. 5c - 11c, also belongs to the same class of events, being predictable, and showing L-shaped statistics. In this regime, the detuning from the degenerate state was larger than in the previously illustrated case.

Downloaded From: https://www.spiedigitallibrary.org/conference-proceedings-of-spie on 11/2/2017 Terms of Use: https://spiedigitallibrary.spie.org/ss/TermsOfUse.aspx

While the detuning from the partially degenerate state was getting larger, we have observed different harmonics. All these regimes were classified to the same class of periodical, predictable events with L-statistics. Meanwhile, these high harmonics were observed in the oscilloscope trace, the fourth and fifth eigenfrequencies (ν_3 of 360-380 Hz and ν_4 of 95-110 Hz respectively) become more visible.

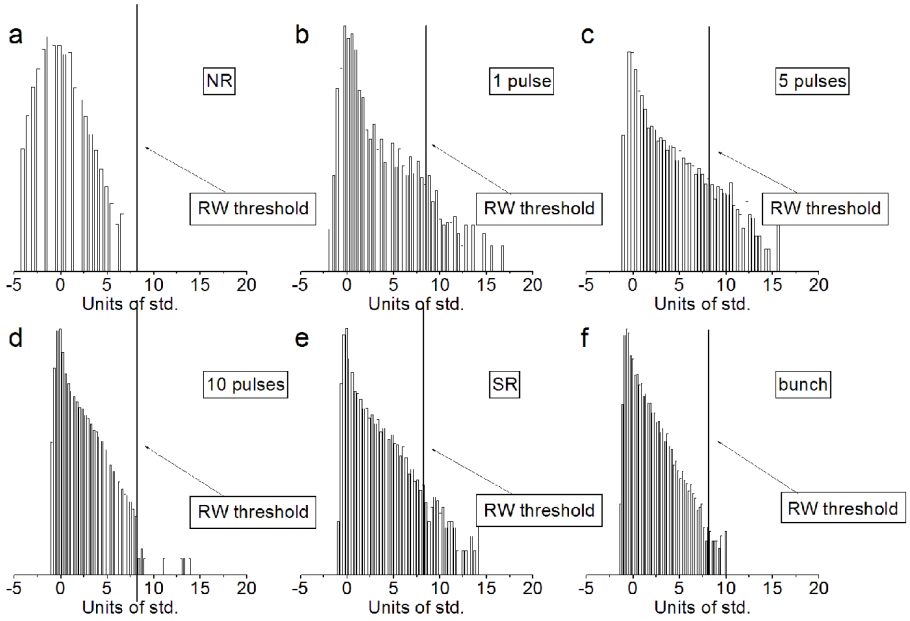

Figure 11. PDFs, depicted in logarithmic scale, for the regimes of interest, case (a) corresponds to partial degeneration, meanwhile cases (b-f) to non-degenerate regimes. The vertical line marks RW thresholds.

Table 1. Dominant Lyapunov Exponents 10.

Regime	NR	1 pulses	5 pulses	10 pulses	SR	Bunch
Filter 1 MHz	0.35	3.135	0.6010	1.4870	2.5910	1.4280
Filter 2.5 GHz	42	28	42	168	393	228
Rogue waves	No	No	No	No	Yes	Yes
L-shaped histogram	No	Yes	Yes	Yes	Yes	Yes
Noise pump modulation	Yes	Yes	Yes	Very high	Very high	Very high
Chaos in a filtered signal	Yes	Yes	Yes	Yes	Yes	Yes

The regime illustrated in Figs. 5e - 11e (labeled with "SR") corresponds to the situation when we have observed mostly slow RW events (11, 12). This regime was observed when the knobs of PC1 and PC2 were set at 20° and 40° from the vertical position, respectively. In this regime, the signal also has L-shaped statistics, but in difference with the previously illustrated regimes, two very small peaks (ν_5 of $\tilde{3}0$ Hz and ν_6 of $\tilde{2}4$Hz) were observed in RF spectra (Fig. 3). Bunches of 15 pulses per period have similar to a soliton rain appearance. However, the positions of pulses were practically periodic during thousands of round trips as the pulses were

Downloaded From: https://www.spiedigitallibrary.org/conference-proceedings-of-spie on 11/2/2017 Terms of Use: https://spiedigitallibrary.spie.org/ss/TermsOfUse.aspx

drifting very slowly. This difference from the soliton rain previously illustrated in the literature 13, probably can be explained by the long-term "memory" in the system due to periodic amplification of the pulses. This periodic amplification in absence of a saturable absorber impedes to a pulse easily change its relative positions in the cavity. Hence, the signal was not periodic at large time scale and these events finally were classified as a true slow RW events (11, 12)).

The last regime illustrated in Figs. 5f - 11f (labeled with "Bunch") was a regime where we mostly observed fast RWs 1. In this regime, all seven eigenfrequencies were observed in the RF spectra (Fig. 11f). Moreover, the optical spectra were split into two peaks (Fig. 7f) revealing the existence of two polarizations in the cavity. This regime corresponded to the completely non-degenerate case. The Stokes parameters (Figs. 8f - 10f) were evolving periodically with frequency ν_0.

5. CONCLUSIONS

In conclusion, we have experimentally investigated transition between chaotic noise operation with quasi-Gaussian PDF and chaotic multi-pulsing regime with L-shaped PDF in a passively self-mode-locked erbium-doped fiber oscillator implemented in a ring configuration and operating near the lasing threshold. We confirmed the existence of seven eigenfrequencies predicted by the theoretical model. Using in-cavity polarization controller we changed the birefringence in the cavity and excite different sets of eigenfrequencies.

Chaotic noisy oscillations observed for degenerate regime evolved to true RW regime through partially mode-locked regimes with L-shaped PDF. The fact that further extinction of eigenfrequencies leads to noisy regimes, previously, was not predicted by the existing theoretical approach. Although, similar regimes in networks were previously discussed in the literature (see for example Refs. [55, 61, 224 and 231] and Fig.34 in 14).

ACKNOWLEDGMENTS

Authors acknowledge support from the Leverhulme Trust (Grant ref: RPG-2014-304), FP7-PEOPLE-2012-IAPP (project GRIFFON, No. 324391).

REFERENCES

[1] Kolpakov, S. A., Kbashi, H., and Sergeyev, S. V., "Dynamics of vector rogue waves in a fiber laser with a ring cavity," *Optica* **3**, 870–875 (Aug 2016).

[2] Sorensen, S. T., Bang, O., Wetzel, B., and Dudley, J. M., "Describing supercontinuum noise and rogue wave statistics using higher-order moments," *Optics Communications* **285**(9), 2451 – 2455 (2012).

[3] Lecaplain, C. and Grelu, P., "Rogue wave statistics from a noise-like-pulse laser," in [*Advanced Photonics*], *Advanced Photonics* , NM3A.7, Optical Society of America (2014).

[4] Stöckmann, H.-J. and Stein, J., ""quantum" chaos in billiards studied by microwave absorption," *Phys. Rev. Lett.* **64**, 2215–2218 (May 1990).

[5] Dörr, U., Stöckmann, H.-J., Barth, M., and Kuhl, U., "Scarred and chaotic field distributions in a three-dimensional sinai-microwave resonator," *Phys. Rev. Lett.* **80**, 1030–1033 (Feb 1998).

[6] Agam, O., Altshuler, B. L., and Andreev, A. V., "Spectral statistics: From disordered to chaotic systems," *Phys. Rev. Lett.* **75**, 4389–4392 (Dec 1995).

[7] Barnett, A., "Asymptotic rate of quantum ergodicity in chaotic euclidean billiards," *Communications on Pure and Applied Mathematics* **59**(10), 1457–1488 (2006).

[8] Sergeyev, S. V., Kbashi, H., Tarasov, N., Loiko, Y., and Kolpakov, S. A., "Vector-resonance-multimode instability," *Phys. Rev. Lett.* **118**, 033904 (Jan 2017).

[9] Lecaplain, C., Grelu, P., and Wabnitz, S., "Dynamics of the transition from polarization disorder to antiphase polarization domains in vector fiber lasers," *Phys. Rev. A* **89**, 063812 (Jun 2014).

[10] Wolf, A., Swift, J. B., Swinney, H. L., and Vastano, J. A., "Determining lyapunov exponents from a time series," *Physica D: Nonlinear Phenomena* **16**(3), 285 – 317 (1985).

[11] Kolpakov, S., Kbashi, H., and Sergeyev, S., "Slow optical rogue waves in a unidirectional fiber laser," in [*Conference on Lasers and Electro-Optics*], *Conference on Lasers and Electro-Optics* , JW2A.56, Optical Society of America (2016).

Downloaded From: https://www.spiedigitallibrary.org/conference-proceedings-of-spie on 11/2/2017 Terms of Use: https://spiedigitallibrary.spie.org/ss/TermsOfUse.aspx

[12] Kbashi, H., Kolpakov, S., and Sergeyev, S., [*Temporal scaling of optical rogue waves in unidirectional ring fiber laser*], IEEE, United States (8 2016). 2016 IEEE. Personal use of this material is permitted. Permission from IEEE must be obtained for all other uses, in any current or future media, including reprinting/republishing this material for advertising or promotional purposes, creating new collective works, for resale or redistribution to servers or lists, or reuse of any copyrighted component of this work in other works.

[13] Chouli, S. and Grelu, P., "Rains of solitons in a fiber laser," *Opt. Express* **17**, 11776–11781 (Jul 2009).

[14] Arenas, A., Daz-Guilera, A., Kurths, J., Moreno, Y., and Zhou, C., "Synchronization in complex networks," *Physics Reports* **469**(3), 93 – 153 (2008).

Downloaded From: https://www.spiedigitallibrary.org/conference-proceedings-of-spie on 11/2/2017 Terms of Use: https://spiedigitallibrary.spie.org/ss/TermsOfUse.aspx